

3D Finite Element Model and Measurement Comparison for Roller Compaction Induced Vibration: The Case Study of a Ring Road in Hanoi, Vietnam

Ngoc Long Nguyen

University of Transport and Communications, Vietnam
nguyenngoclong@utc.edu.vn

Chau Lan Nguyen

University of Transport and Communications, Vietnam
nguyenchaulan@utc.edu.vn (corresponding author)

Tien Thanh Bui

University of Transport and Communications, Vietnam
btthanh@utc.edu.vn

Hong Lam Dang

University of Transport and Communications, Vietnam
dang.hong.lam@utc.edu.vn

Received: 29 May 2023 | Revised: 17 June 2023 | Accepted: 24 June 2023

Licensed under a CC-BY 4.0 license | Copyright (c) by the authors | DOI: <https://doi.org/10.48084/etasr.6070>

ABSTRACT

Vietnam is currently constructing many transportation and infrastructure projects in urban areas. During the construction process of road foundations such as pile driving and vibratory compaction often causes vibrations that can affect nearby structures. Therefore, it is necessary to study the impact of vibrations induced by construction activities. A study was conducted to investigate the impact of roller compaction-induced vibration on the buildings and structures of Ring Road No.2 in Hanoi, Vietnam. The study also applied a 3D FEM method to evaluate the impact of vibration on surrounding structures. The results showed a good correlation between finite element calculations and field measurements.

Keywords-3D Plaxis; vibration; FEM; soil structure dynamics

I. INTRODUCTION

The construction of Ring Road No.2 in Hanoi was executed in 2018 and consisted of two sections: an elevated section and a lower section. The elevated section is over 5 km long, starting from the southern connection point of Vinh Tuy Bridge and ending at the intersection with Nga Tu So Street. The lower extension, which links to Vinh Tuy Bridge at the starting point, is approximately 3 km long and terminates at the Nga Tu Vong intersection. This is a road with high traffic density, and there are many buildings around it. The use of vibrating rollers for road foundation construction raises concerns about their impact on nearby buildings and historic structures. Therefore, it is necessary to assess and monitor the effects of this construction activity on the structures placed along the Ring Road No.2.

Construction activities in city sites can cause significant disturbances to nearby structures such as differential settlement, even collapse [1-5]. The vibration sources are soil excavation, pile driving, and compaction using vibratory equipment [2-4, 6-10]. These sources can cause vibrations in the surrounding soils, which will be transmitted to nearby buildings and structures. For example, a resonance in multi-story buildings at distances close to 200 and 500 m from dynamic sources was observed. In addition, a frequency of 26 Hz from a vibratory sheet pile can generate ground vibrations below 5 mm/s and vertical floor vibrations higher than 51 mm/s in two-story houses and can cause architectural damage [11]. The impact of these vibrations on existing structures is typically measured by particle vibration velocity. Most standards and guidelines set an allowable vibration level based on Peak Particle Velocity (PPV) [12, 13]. BS 5228: Part 4:

1992, which is a code of practice for managing noise and vibration during piling operations, also offers direction on the permissible levels of vibration in structures. According to this standard, a cautious limit of PPV for intermittent vibration should be set at 10 mm/s, while for continuous vibrations it should be 5 mm/s, to avoid minor or cosmetic damage [6].

Experimental and numerical analysis are commonly used to solve wave propagation induced by impact pile driving [4, 7, 8, 14-17]. Authors in [18] performed a 2D numerical analysis to estimate the soil deformation induced by vibrations of the piling hammer. Authors in [15] evaluated the seismic loading of nearby structures according to the Czech technical standards. Authors in [6] focused on the study of field monitoring of roller vibrations during the compaction of subgrade soil. Previous studies in Vietnam have investigated the effects of construction vibrations on buildings and structures [19, 20]. Authors in [21] focused on controlling vibrations on existing buildings in the Metro Line 3 project. The monitoring and numerical analysis (Plaxis 3D) results showed the minimum distance of 4 m between the vibration source and the existing building and the grab drop height of 1 m of grab shock for the Metro Line 3 project. However, other construction activities, such as vibrating rollers, have not been studied carefully regarding the effect on nearby buildings on the construction site in Hanoi. Therefore, this study aims to use the Finite Element Method (FEM) to address wave propagation in non-homogeneous ground conditions in Hanoi due to a vibrating roller, and to compare the results obtained from the FEM with the experimental data of the Ring Road No.2 construction project.

II. METHOD

A. Soil Investigation

The geological soil profile of Borehole 1, which is close to the measurement points, is shown in Figure 1. For a detailed geological investigation, Standard Penetration Tests (SPTs) were conducted at every 2 m depth. It is observed that the stratigraphy consists of 7 layers. The 1st layer is filled soil (layer 1) with thickness of about 1.2 m. Below, there is a yellow/brown soft to medium sandy clay (CL) layer with an average thickness of 4.4 m and uncorrected $N_{spt} = 6\sim 16$. The 3rd layer is fine sand (layer 3) with about 1.2 m thickness. The 4th layer is also yellow/brown, soft sandy clay (CL) with a thickness of about 3.7 m and uncorrected $N_{spt} = 5\sim 6$. Layer 5 is brown soft sandy clay (CL) with some gravels (layer 5), with thickness of 10.8 m and $N_{spt} = 10\sim 23$. The 6th layer is also yellow/brown, soft sandy clay (CL) with a thickness of about 7.5 m and uncorrected $N_{spt} = 8\sim 11$. The 7th layer is also yellow/brown, stiff sandy clay (CL) with a thickness of about 7.5 m and uncorrected $N_{spt} = 14\sim 15$.

Soil samples were retrieved for the conduction of laboratory tests, such as physical property tests (water content, soil distribution, Atterberg limit, etc.) and mechanical property tests (consolidation test, hydraulic conductivity test, triaxial test). The physical and mechanical properties results for soil layers were collected and were considered as input parameters for Plaxis 3D model. They are presented in Table I.

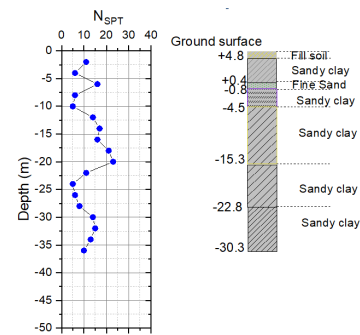


Fig. 1. SPT value for soil profile in Borehole 1.

TABLE I. SOIL PARAMETERS IN PLAXIS 3D

Contents	Layer 1	Layer 2	Layer 3	Layer 4	Layer 5	Layer 6	Layer 7
Type of model	MC						
Unit weight γ (kN/m ³)	18	18.6	13.4	19	17.3	19.7	18
Saturated unit weight γ_{sat} (kN/m ³)	18.5	18.68	13.84	19.5	17.3	19.89	18.5
Cohesion, c' (kPa)	15	23	8.8	1	15.8	27.3	20
Friction angle, ϕ' (°)	20	12.91	8.18	28.23	18.5	15.76	20
ν	0.32	0.3	0.3	0.3	0.3	0.3	0.3
E_{oed} (MPa)	21.46	26.92	4.815	40.38	21.46	26	26.92
E (MPa)	15	20	3.0	30	15	26	20
V_s (m/s)	55.65	63.7	28.52	77.18	56.76	80.46	64.75
V_p (m/s)	108.2	119.2	59.37	144.4	110.3	113.8	121.1
R_{inter}	0.65	0.7	0.7	0.7	0.65	0.8	0.65

Note: c' and ϕ' are taken from the consolidated undrained triaxial test.

B. Monitoring

Accelerometers or geophones can be utilized to measure the vibration velocity (PPV) in mm/s and assess the impact of construction activities on a plane that requires compaction using a vibrating roller [6, 7]. The vibrating roller HAMM 20T generates vibrations with a frequency range of 27 Hz to 30 Hz and applies a centrifugal force of 250 kN to 330 kN (Figure 2). The significant impact produced by the roller compaction can cause soil particles to displace and compress, leading to a reduction in soil porosity and resulting in ground vibrations that may affect nearby structures. To determine the magnitude of the impact caused by the roller compaction vibrations, acceleration sensors placed on steel anchors were used to record the ground's dynamic response during the construction process. The devices used for vibration monitoring are depicted in Figure 3. Four sensors, namely 31, 32, 35, and 36 were used in this study with highly sensitive accelerometers and vibration detection sensors. Sensors 31 and 35 monitored vertical acceleration, while sensors 32 and 36 measured horizontal acceleration for point 1 and point 2, respectively. The measuring frequency range of the sensors is 0.15 ÷ 1000 Hz. The sensitivity of the sensors is approximately 10000 mV/g equal to 1019.4 mV/(m/s²) and their non-linearity is less than 1%.



Fig. 2. Vibration source - HAMM 20T.

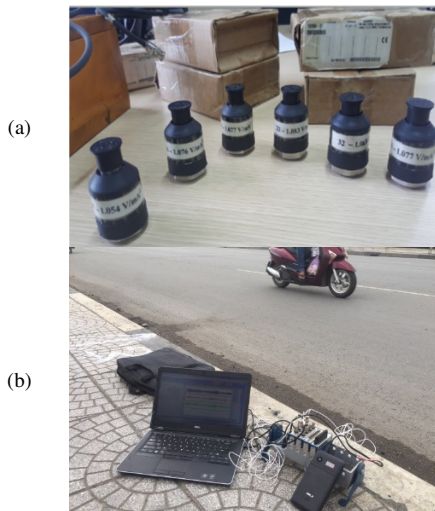


Fig. 3. Test setup: (a) Acceleration sensors, (b) data acquisition and computer analysis.

The vibrating work was carried out along the road. The experiment was conducted to measure ground vibration for a 3-story building (Figure 4). The distance from the vibration machine to point 1 and point 2 are shown in Figure 1. The vibration measuring device was attached to a 30 cm length of steel pile at the foundation of the building. During the operation of the roller compactor, vibration measurements were taken. Then, the measured data were processed and analyzed with the Elasto-Dynamic program for comparison and evaluation.

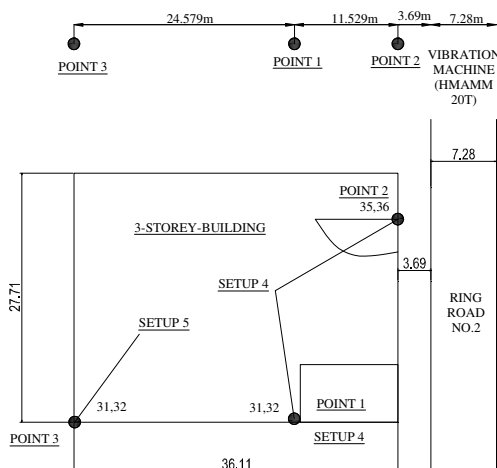


Fig. 4. Monitoring point setup for a 3-story building.

C. 3D Plaxis Model

In this study, the wave propagation from roller compaction was modeled with Plaxis 3D dynamic finite element code. The dimensions of the model is shown in Figure 5. Soil conditions and shear wave velocity are included in the model (Table I) with the profile shown in Figure 1. The soil layers were modeled using the Mohr-Coulomb (MC) model in Plaxis with the input parameters presented in Table I. The transversal and longitudinal seismic wave propagation velocities were automatically determined in Plaxis 3D by:

$$v_p = \sqrt{\frac{E_{oed}}{\rho}} = \sqrt{\frac{G(2-2\nu)}{\rho(1-2\nu)}} \tag{1}$$

$$v_s = \sqrt{\frac{G}{\rho}} \tag{2}$$

The three-story building was modeled with plate elements. Its input parameters are presented in Table II.

TABLE II. INPUT PARAMETERS FOR 3-STORY BUILDING IN PLAXIS 3D

Contents	Unit	
Type of model	-	Elastic
γ	kN/m ³	24.5
$E1$	kPa	26+E6
$E2$	kPa	26+E6
$G12$	kPa	11.67+E6
ν_{12}	-	0.2

The Plaxis 3D has a calculation dynamic module that allows for solving dynamic problems using FEM. The elementary equation for calculating time-dependent deformation changes under dynamic loading in matrix notation for the entire area under consideration is:

$$F = F' M' \sin(\omega t + \varphi_0) \tag{3}$$

where M' is the amplitude multiplier, F' is the input value of the load, $\omega = 2\pi f$ with f being the frequency in Hz, φ_0 is the initial phase angle, and $F'M'$ is the amplitude of the dynamic load. For HAMM 20T vibrating roller, the $F'M'$ is taken as 330 kN, the frequency is obtained as $f=30$ Hz and the initial phase angle is equal to 0.

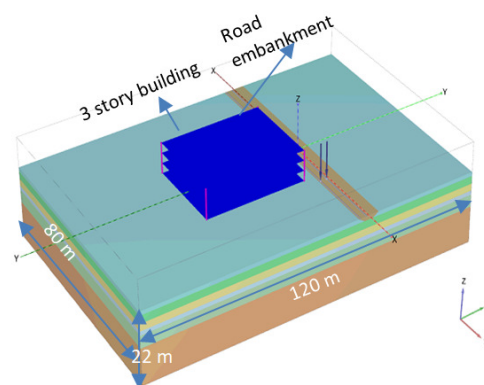


Fig. 5. Plaxis 3D model of a 3-story building.

III. RESULTS

A. Monitoring Results

The obtained vibration velocities are shown in Figures 6-9.

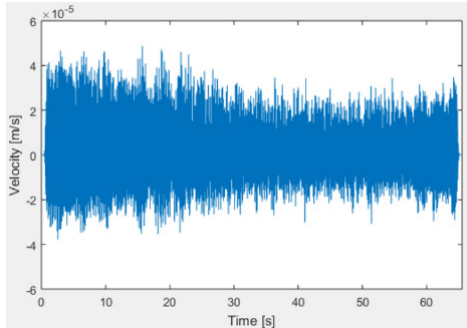


Fig. 6. Vertical velocity versus dynamic time at point 31.

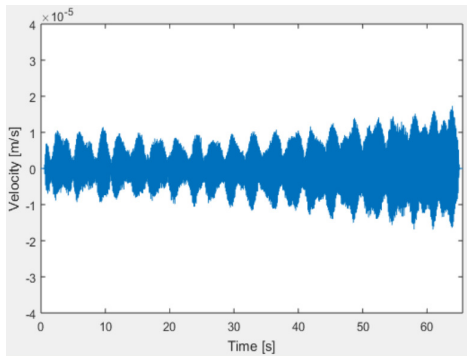


Fig. 7. Horizontal velocity versus dynamic time at point 32.

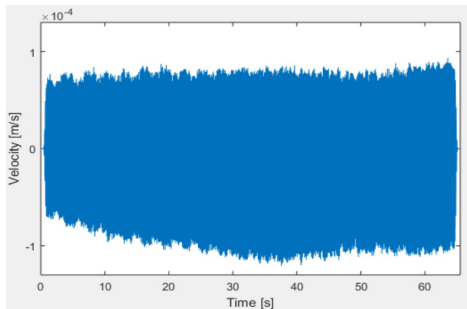


Fig. 8. Vertical velocity versus dynamic time at point 35.

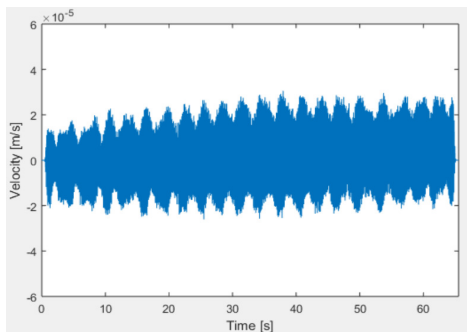


Fig. 9. Horizontal velocity versus dynamic time at point 36.

B. Plaxis 3D Results

The vibration velocities obtained from Plaxis 3D are shown in Figures 10-13.

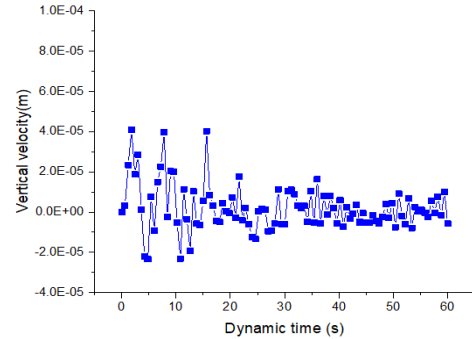


Fig. 10. Vertical velocity versus dynamic time at point 31.

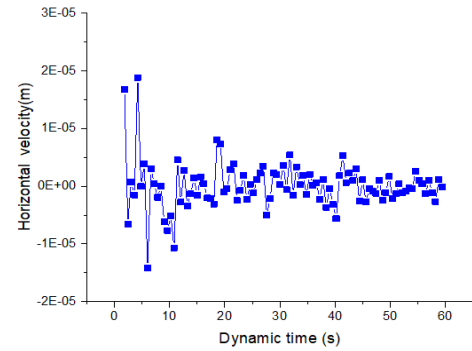


Fig. 11. Horizontal velocity versus dynamic time at point 32.

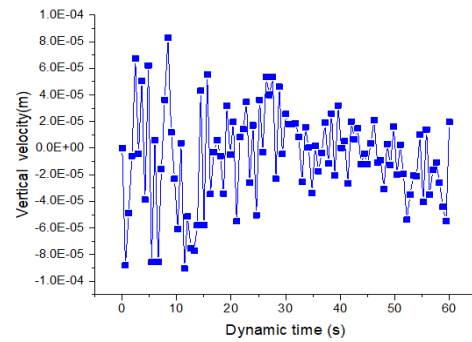


Fig. 12. Vertical velocity versus dynamic time at point 35.

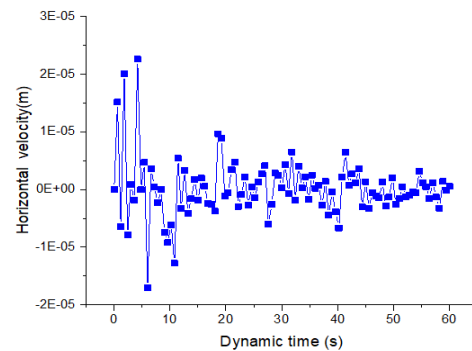


Fig. 13. Horizontal velocity versus dynamic time at point 36.

The monitoring data and 3D Plaxis results are summarized in Table III.

TABLE III. COMPARISON OF MONITORING DATA AND FEM 3D RESULTS

Point	Vibration direction	Distance to the vibration source (m)	Monitoring data PPV (m/s)	FEM 3D PPV (m/s)
S32	Horizontal	3.7	4×10^{-5}	4.1×10^{-5}
S31	Vertical	3.7	1.8×10^{-5}	1.88×10^{-5}
S35	Vertical	12.5	8.5×10^{-5}	8.3×10^{-5}
S36	Horizontal	12.5	2.5×10^{-5}	2.3×10^{-5}

The waveform records of the vibration velocities (horizontal component v_x , and v_y , vertical component v_z) are shown in Figures 10-13. The maximum vertical velocity (v_z), as can be seen in Table III, is about 8.5×10^{-5} mm/s. This finding is consistent with previous research [2, 5, 6]. It is observed that the maximum measured velocity values were similar to the values derived from the numerical analysis. Normally, the maximum PPV for buildings and structures with masonry or concrete construction should not exceed 12.5 mm/s for short-term exposures and 5 mm/s for long-term exposures. Similarly, the International Organization for Standardization (ISO) recommends a maximum PPV of 10 mm/s for buildings and structures. Therefore, the PPV value is still lower than standard requirements, which means that the house still is not affected by vibrations induced by roller compaction in this case.

Figure 14 presents the vertical displacement of the soil due to the vibration of the roller. A small value of displacement was observed and it had no effect on the settlement of the house.

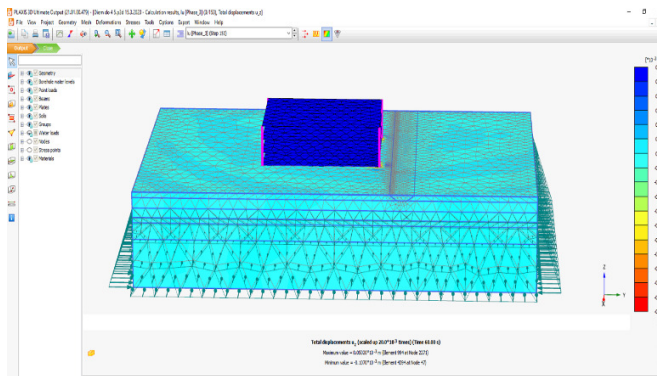


Fig. 14. Vertical displacement due to roller vibration.

IV. CONCLUSION

This paper presents the results of experimental measurements and 3D FEM modeling of the roller compaction effects during the construction of the Ring Road No.2 in Hanoi, Vietnam. The FEM dynamic analysis (Plaxis 3D) of roller compaction-induced vibration based on the Hanoi conditions was studied. The results show that the velocity decreases with the increase in distance from the roller. The FEM results are in good agreement with the actual velocity measurements and frequency dominant structure responses due to ground-borne vibration.

ACKNOWLEDGMENT

This research is funded by the University of Transport and Communications (UTC) under grant number T2022-CT-009TĐ.

REFERENCES

- [1] M. E. Bayraktar, Y. Kang, M. Svinikin, and F. Arif, "Evaluation of Vibration Limits and Mitigation Techniques for Urban Construction," Florida Department of Transportation, Tallahassee, FL, USA, FDOT Contract No.: BDK80 977-22, Oct. 2013.
- [2] S. Ouakka, O. Verlinden, and G. Kouroussis, "Railway ground vibration and mitigation measures: benchmarking of best practices," *Railway Engineering Science*, vol. 30, no. 1, pp. 1–22, Mar. 2022, <https://doi.org/10.1007/s40534-021-00264-9>.
- [3] V. Leggieri, A. di Lernia, G. Elia, D. Raffaele, and G. Uva, "Vibrations Induced by Mechanical Rock Excavation on R.C. Buildings in an Urban Area," *Buildings*, vol. 11, no. 1, Jan. 2021, Art. no. 15, <https://doi.org/10.3390/buildings11010015>.
- [4] F. Deckner, "Ground vibrations due to pile and sheet pile driving – influencing factors, predictions and measurements," Licentiate thesis, Royal Institute of Technology, Stockholm, Sweden, 2013.
- [5] B. Mazouz, T. Mansouri, M. Baazouzi, and K. Abbeche, "Assessing the Effect of Underground Void on Strip Footing Sitting on a Reinforced Sand Slope with Numerical Modeling," *Engineering, Technology & Applied Science Research*, vol. 12, no. 4, pp. 9005–9011, Aug. 2022, <https://doi.org/10.48084/etasr.5131>.
- [6] P. D. Cenek, A. J. Sutherland, and I. R. McIver, "Ground vibration from road construction," NZ Transport Agency, New Zealand Transport Agency research report 485, May 2012.
- [7] M. A. Mooney and R. V. Rinehart, "Field Monitoring of Roller Vibration during Compaction of Subgrade Soil," *Journal of Geotechnical and Geoenvironmental Engineering*, vol. 133, no. 3, pp. 257–265, Mar. 2007, [https://doi.org/10.1061/\(ASCE\)1090-0241\(2007\)133:3\(257\)](https://doi.org/10.1061/(ASCE)1090-0241(2007)133:3(257)).
- [8] A. Herbut, M. M. Khairutdinov, C. Kongar-Syuryun, and J. Rybak, "The surface wave attenuation as the effect of vibratory compaction of building embankments," *IOP Conference Series: Earth and Environmental Science*, vol. 362, no. 1, Aug. 2019, Art. no. 012131, <https://doi.org/10.1088/1755-1315/362/1/012131>.
- [9] F. Bouabdallah, K. Goudjil, and S. Messast, "The Effect of Rigid Inclusions on the Dynamic Response of Highway Embankment," *Engineering, Technology & Applied Science Research*, vol. 13, no. 1, pp. 9843–9848, Feb. 2023, <https://doi.org/10.48084/etasr.5400>.
- [10] A. S. Jawad and B. S. Albusoda, "Numerical Modeling of a Pile Group Subjected to Seismic Loading Using the Hypoplasticity Model," *Engineering, Technology & Applied Science Research*, vol. 12, no. 6, pp. 9771–9778, Dec. 2022, <https://doi.org/10.48084/etasr.5351>.
- [11] M. R. Svinikin, "Minimizing Construction Vibration Effects," *Practice Periodical on Structural Design and Construction*, vol. 9, no. 2, pp. 108–115, May 2004, [https://doi.org/10.1061/\(ASCE\)1084-0680\(2004\)9:2\(108\)](https://doi.org/10.1061/(ASCE)1084-0680(2004)9:2(108)).
- [12] *Vibrations in Building Construction, DIN 4150*. German Standards Organization, 1970.
- [13] *Effects of Vibration on Construction*. Zurich, Switzerland: Swiss Association of Standardization.
- [14] S.-H. Ju, H.-T. Lin, and T.-K. Chen, "Studying Characteristics of Train-Induced Ground Vibrations Adjacent to an Elevated Railway by Field Experiments," *Journal of Geotechnical and Geoenvironmental Engineering*, vol. 133, no. 10, pp. 1302–1307, Oct. 2007, [https://doi.org/10.1061/\(ASCE\)1090-0241\(2007\)133:10\(1302\)](https://doi.org/10.1061/(ASCE)1090-0241(2007)133:10(1302)).
- [15] T. Petrik, M. Lednicka, Z. Kalab, and E. Hrubesova, "Analysis of Technical Seismicity in the Vicinity of Reconstructed Road," *Transactions of the VSB- Technical University of Ostrava*, vol. 12, no. 1, 2012, Art. no. 1.
- [16] A. Amorosi, D. Boldini, and G. Elia, "Parametric study on seismic ground response by finite element modelling," *Computers and*

- Geotechnics*, vol. 37, no. 4, pp. 515–528, Jun. 2010, <https://doi.org/10.1016/j.compgeo.2010.02.005>.
- [17] T. Petrik, E. Hrubešová, and M. Lednická, "A Comparison of Numerical Models Results with in-Situ Measurement of Ground Vibrations Caused by Sheet Pile Driving," *Acta Geodynamica et Geomaterialia*, vol. 9, no. 2, pp. 165–171, 2012.
- [18] F. Syarif, M. Kurniawan, and Elizar, "Soil deformation analysis by using plaxis 2D that cause by vibration of pilling hammer," *IOP Conference Series: Earth and Environmental Science*, vol. 519, no. 1, Mar. 2020, Art. no. 012053, <https://doi.org/10.1088/1755-1315/519/1/012053>.
- [19] N. C. Giang, S. Nishiyama, and Y. Kohata, "Characteristics of Traffic Induced vibration of Ground Filled with Liquefied Stabilized Soil Made from Excavated Vinh Phuc Clay in Hanoi City, Vietnam," *International Journal of Civil Engineering and Technology*, vol. 11, no. 4, pp. 36–53, Apr. 2020.
- [20] N. T. C. Nhung and Q. M. Tran, "The effects of ground vibration induced by construction activities of urban railways in Hanoi," *Journal of Materials and Engineering Structures*, vol. 7, no. 4, pp. 703–710, Dec. 2020.
- [21] H.-L. Dang, V.-Q. Nguyen, and T.-H.-M. Vo, "A study of 3D modelling the vibrations induced from grab shock at the Metro Line 3 project in Hanoi," *Journal of Materials and Engineering Structures*, vol. 9, pp. 557–562, 2022.